Poly(ethylene oxide) Grafted to Silicon Surfaces: Grafting Density and Protein Adsorption

Susan J. Sofia,* V. Premnath, and Edward W. Merrill

Department of Chemical Engineering, Massachusetts Institute of Technology, Cambridge, Massachusetts 02139

Received July 9, 1997; Revised Manuscript Received April 16, 1998

ABSTRACT: Poly(ethylene oxide) (PEO) polymer, in linear and star form, was covalently grafted to silicon surfaces, and the surfaces were tested for their ability to adsorb proteins. Linear PEG of molecular weight 3400, 10 000, and 20 000 g/mol and star PEO molecules were coupled via their terminal hydroxyl groups activated by tresyl chloride to aminosilane-treated silicon wafers. The amount of PEO coupled to the surface was varied by changing the concentration of the tresyl-PEO solution. The dry PEO thickness on the surface was measured using X-ray photoelectron spectroscopy (XPS) and ellipsometry, from which the grafting density was calculated. The PEO surfaces were exposed to solutions of each of three proteins: cytochrome-*c*, albumin, and fibronectin. The degree of adsorption of each protein was determined by XPS and ellipsometry and recorded as a function of PEO grafting density. All three proteins were found to reach zero adsorption at the highest grafting densities on all three PEG surfaces, which for all three PEG surfaces was a PEO content of 100 ± 10 ng/cm^2. On both star PEO surfaces, albumin and fibronectin decreased to zero adsorption at intermediate values of grafting density, whereas cytochrome-*c* continued to adsorb at all grafting densities, although with a decreasing trend. A physical model of the surface helped explain these protein adsorption results in terms of the spacing and degree of overlap of grafted PEO chains.

Introduction

Poly(ethylene oxide) (PEO) is gaining wide recognition as a biomaterial due to its noninteraction with proteins and cells.[1,2] As a result, there have been many attempts to create PEO surfaces for use in biomedical applications. The accurate experimental characterization of these surfaces has traditionally been difficult to accomplish. This is mainly due to the fact that the surfaces on which the PEO was grafted[3−9] or into which PEO was incorporated[10−15] were polymers**,** and polymers can have very rough, nonuniform, and dynamic surfaces that make their accurate characterization quite a challenge. The use of X-ray photoelectron spectroscopy (XPS) or secondary ion mass spectrometry (SIMS) has traditionally been used, but these techniques mainly reveal qualitatively the PEO content on the surface. A direct experimental correlation of biological interactions with PEO surface content had not yet been achieved. At best, the efficacy of these surfaces was usually determined by observing the extent of biological interaction with them and then correlating these interactions with the PEO characteristics, such as PEO molecular weight and PEO content in the material, but not specifically with the amount of PEO present on the surface. In our work on silicon wafers presented in this paper, we were able to determine the amount of PEO on the surface and, through a surface model, to correlate protein adsorption with PEO surface content, molecular weight, molecular form (star-shaped or linear random coil), and protein size.

In one experimental approach, Prime and Whitesides[16] characterized protein adsorption on surfaces of varying poly(ethylene glycol) (PEG) content and molecular weight achieved with self-assembled monolayers (SAMs) on gold substrates. (We use PEG in place of PEO when referring to molecular weights below 25 000 g/mol.) These self-assembled monolayer surfaces can be characterized very accurately with techniques such as ellipsometry, XPS, and ATR-FTIR, to name a few.[16,17] This study showed convincingly that only very short lengths of PEO (PEGs of only 2−6 monomer units) can succeed, at sufficient densities, at preventing protein adsorption, which dispels the notion that very small molecular weight PEG loses its "ability" to repel proteins.[9] However, the question of what grafting densities are required for longer, randomly coiling PEG chains has still not been fully answered. The method of assembling the PEG SAMs is very well defined and specific to gold, on which very high grafting densities can be achieved. The grafting of randomly coiling molecules, on the other hand, typically results in a maximum grafting density at the onset of a brush regime, that is, chain spacings roughly equaling the radius of gyration of the grafted chain such that the chains begin to stretch away from the surface.[18−21] We wanted to specifically test for protein adsorption behavior in this range of experimentally achievable grafting densities of PEO molecules.

Several theoretical approaches have been investigated in trying to gain a better understanding of protein−polymer interactions.[21−25] Jeon et al.[22] modeled the protein resistance of a grafted PEO surface through a combination of hydrophobic interactions, Van der Waals attractions, and steric repulsion of the grafted PEO chain as it is compressed by an approaching protein. In their studies, they concluded that both density and chain length are important in rejecting proteins, with the former have a greater importance. However, the surface conditions that were investigated were PEO chains in a dense brush layer, which as stated earlier

* Corresponding author. Current address: Department of Chemical Engineering, Tufts University, 4 Colby Street, Medford, MA 02155. Phone: (617) 628-5000 x2670. Fax: (617) 627-3991. E-mail: ssofia@emerald.tufts.edu.

S0024-9297(97)01016-4 CCC: $15.00
Published on Web 07/10/1998

are conditions that are extremely difficult to achieve experimentally. Szleifer,[21] on the other hand, used a generalization of the single-chain mean-field theory to investigate the interaction of a protein (lysozyme) with a hydrated polymer (PEO) surface. In varying the surface coverage (well within the experimental range), the protein configuration, the type of surface, and the molecular weight of the grafted polymer, the effects on the equilibrium adsorption isotherms were then determined. Our results presented here agree fairly well with these findings.

The information presented in this paper provides methods of grafting, adsorption, and analysis that lend some insight into the dependence of protein adsorption on linear and star-shaped PEO-grafted surfaces in a range of PEO grafting densities. Silicon wafers were used as a model substrate material, where the surface is stable and extremely flat. A triaminosilane was covalently coupled to the surface, which provided a high concentration of grafting sites (both primary and secondary amines) for the attachment of the PEO. Tresyl chloride chemistry was used to couple the PEO hydroxyl chain ends to the amines on the surface.

Both linear and star-shaped PEO molecules were grafted to the silicon surfaces in order to study the difference in their grafting densities and their effectiveness at preventing protein adsorption. Linear PEO random coils have a very loose, nondense structure with only two chain ends per molecule. These chain ends could be located anywhere within the volume of the molecule, thus causing its grafting probability to decrease with increasing molecular weight. In contrast, star molecules, having a central core region with PEO arms extending radially from that core, have very dense, hard-sphere character,[26] with a large number of chain ends per molecule that are located at the outer regions of the molecule due to the steric hindrance within the center of the molecule.[27,28] Thus, its probability of grafting to a surface is extremely high and would only decrease with a return to more random-coil characteristics (i.e., with increasing arm molecular weight and/or decreasing functionality).

The PEO surfaces were contacted with protein solutions of cytochrome-*c*, albumin, and fibronectin, and the respective adsorptions were measured. These three proteins were chosen because they span a wide range of sizes, from 12 kD for cytochrome-*c* (spherical in shape, diameter 34 Å), to 68 kD for albumin (spherical in shape, diameter 72 Å), to 500 kD for fibronectin (rodlike shape, 600 Å long and 25 Å wide). This is so adsorption as a function of protein size could also be tested.

Ellipsometry and X-ray photoelectron spectroscopy (XPS) were used to analyze the surfaces after each step in the surface modification. In all cases there was good agreement between the measurements obtained from both methods.

Materials and Methods

Aminosilane Coupling to Silicon. Silicon wafers (100) were obtained from Silicon Sense Inc. (Nashua, NH). Trimethoxysilylpropyldiethylenetriamine ($(MeO)_3Si(CH_2)_3NH(CH_2)_2NH(CH_2)_2NH_2$) was obtained from United Chemical Technologies (Bristol, PA) and used as received. Ultrapure water was provided from a Millipore Inc. (Bedford, MA) RO-60/Milli-Q water purification system (resistance = 18 MΩ·cm). Anhydrous methanol was used as received.

The aminosilane coupling procedure was the same as that used by Stenger et al.[29] Silicon wafer pieces were first cleaned by soaking in a 1:1 (v:v) methanol/concentrated HCl solution for a minimum of 30 min. They were rinsed thoroughly with water and then placed in concentrated sulfuric acid (ca. 96%) for a minimum of 30 min. Once they were rinsed thoroughly with water, they were quickly rinsed in methanol to remove the water. The silane solution consisted of 94% mildly acidified methanol (1 mM acetic acid in methanol), 5% water, and 1% silane by volume. When preparing the silane solution, the silane was first added to the acidified methanol, and the water was added second, 1 mL at a time. The water was added to the solution as soon as possible after the silane, and then the solution was gently mixed and immediately contacted with the silicon. Delays beyond several minutes between these steps can lead to inhomogeneities and inconsistencies in the resulting surface.[29] The silicon pieces were reacted for 15 min in the silane solution, rinsed thoroughly three times with methanol, and then baked in a convection oven at 120 °C for 10−15 min. The wafers were coupled to tresylated PEO no more than 48 h after they were prepared, rinsing them in methanol immediately before coupling.

Tresylation of Linear PEG and STAR PEO. Linear poly(ethylene glycol) (PEG) standards were obtained from Scientific Polymer Products (Ontario, NY), with molecular weights 10 000 g/mol ($\bar{M}_w$ = 9760 g/mol, PDI = 1.05) and 20 000 g/mol ($\bar{M}_w$ = 19800 g/mol, PDI = 1.05). PEG 3400 ($\bar{M}_w$ = 3350 g/mol, PDI = 1.1) was a gift provided by Shearwater Polymers, Inc. (Huntsville, AL). PEO star polymers were a gift from Dr. Pierre Lutz at the Institute Charles Sadron in Strasbourg, France. Two types were used in these studies: #228, $\bar{M}_w$ = 200 000 g/mol, $\bar{M}_{arm}$ = 10 000 g/mol, $\bar{f}$ = 20; #3510, $\bar{M}_w$ = 350 000 g/mol, $\bar{M}_{arm}$ = 5200 g/mol, $\bar{f}$ = 70, where $\bar{f}$ is the average functionality of the star molecule. Trifluoroethanesulfonyl chloride (tresyl chloride, TrCl) and triethylamine (TEA) were obtained from Aldrich Chemical Inc. (Milwaukee, WI). Dichloromethane (CH_2Cl_2) and methanol were used as received.

The tresylation reaction procedure was the same as that published by Nilsson and Mosbach.[30,31] The reaction vessel (100 mL round-bottom flask) with a stir bar was dried in a convection oven at 120 °C for a minimum of 24 h before reaction. The PEO to be tresylated was dissolved in dichloromethane (5−10% w/v, usually 2 g of PEO in 20−25 mL of CH_2Cl_2) before molecular sieves were added. The solution was allowed to finish bubbling while lightly capped, (ca. 30 min) before being sealed and stored at 4 °C for a minimum of 24 h. Molecular sieves were added to a small aliquot (ca. 10 mL) of TEA, which was allowed to bubble and was then sealed and also stored at 4 °C for a minimum of 24 h. It is important that all solutions and glassware involved in the tresylation reaction are as water-free as possible; otherwise, the reaction will not proceed to a high yield.

The PEO/dichloromethane solution was quickly decanted into the reaction vessel, and the stir bar was set to stir at a slow to medium rate. The TEA was pipetted dropwise into the reaction vessel, followed by TrCl. The amounts of TEA and TrCl to be added were determined by first calculating the approximate number of moles of hydroxyl groups present for tresylation (no. of moles of OH = 2(mass PEO added)/($\bar{M}_n$ of PEO)). The number of moles of hydroxyl groups for the star polymer was approximated as (mass of star PEO added)/$\bar{M}_{arm}$. The amount of TEA and TrCl to be added was then 1.5 times the number of moles of OH calculated. The reaction was allowed to proceed for 90 min before the dichloromethane was removed. The polymer was then redissolved in 50 mL of acidified methanol (250 μL of concentrated HCl in 50 mL of methanol) and placed at −20 °C to precipitate the tresylated PEO. The solution was then centrifuged at −20 °C for 25 min, the supernatant poured off, and the PEO redissolved in an additional 50 mL of acidified methanol (*now* 50 μL of concentrated HCl in 50 mL of methanol). The procedure of precipitation, centrifugation, and redissolving in 50 mL of acidified methanol (50 μL of concentrated HCl in 50 mL of methanol) was repeated until a total of four precipitations were performed (at least six if sent out for elemental analysis). Once the polymer was recovered from the last centrifugation and the

methanol removed, the tresylated polymer either was used immediately or was stored under nitrogen, dessicated, at −70 °C. When a sample of a tresylated PEG 3400 standard was sent out for elemental analysis (Galbraith Labs, Knoxville, TN), the yield was found to be 75−80%.

Coupling Tresyl-PEO to Aminosilane−Silicon Surfaces. Varying amounts of tresylated-PEO were added to 3 mL of sodium bicarbonate buffer solution (0.12 M, pH 7.4). Immediately after the polymer dissolved fully, the pieces of aminosilane-treated silicon were added. The silicon pieces were kept in the solution overnight, at 25 °C on a rocker table, before being removed and rinsed thoroughly with water. This ensured the greatest extent of reaction on the surface and that all unreacted tresyl groups were hydrolyzed off to restore the hydroxyl groups on the PEO. Concentrations of tresyl-PEO ranged from 0.05% to 15% (w/v) for the star PEOs and 0.05% to 19% (w/v) for the linear PEGs. Generally, six different concentrations were prepared for each PEO sample, and two samples were made at each concentration.

Protein Adsorption. The proteins cytochrome-*c* (equine, MW = 12 kD), albumin (human, MW = 68 kD), and fibronectin (human, MW = 500 kD) were obtained from Sigma Chemical (St. Louis, MO), as was phosphate-buffered saline (PBS) solution (0.01 M phosphate, 0.1 M NaCl, pH 7.4). Sodium azide (0.02% w/v) was added to the PBS solution to act as a bacteriostat. The proteins were dissolved in the PBS at the concentrations 2 mg/mL for cytochrome-*c* and albumin and 0.1 mg/mL for fibronectin. PEO-coupled pieces were rinsed in PBS to rehydrate the surface and then placed in the protein solutions. Adsorption took place at 25 °C for 24 h. Samples were then removed from the solution, gently rinsed three times with approximately 1.5 mL of PBS from a Pasteur pipet for each rinse, and rinsed once with several drops of pure wate to remove PBS salts from the samples.

Analytical Techniques. (a) Ellipsometry. A Gaertner L116a ellipsometer was used to make the thickness measurements on the silicon wafer pieces. Baseline substrate values were taken immediately after the acid-cleaned silicon pieces were rinsed the final time in water and methanol. A nitrogen stream was used to dry the methanol from the surface. A value of 1.44 was used for the index of refraction (*n*) for all measurements. This is a good estimate for the aminosilane[29] and PEO[17] layers. For the protein layer, however, it is only an average value, as *n* for proteins can vary widely depending on several factors.[16] Total thickness measurements were made after each step of coupling with aminosilane, coupling with PEO, and adsorption of protein. Therefore, a single layer thickness (e.g., PEO layer only) was taken to be the difference between the total thickness measurement after the last step (i.e., coupling with PEO) and the thickness measurement from the previous step (i.e., coupling of aminosilane). For all silicon samples, five to eight measurements were made on each sample.

(b) X-ray Photoelectron Spectroscopy (XPS). An SSX-100 X-ray photoelectron spectrometer, which has a monochromatized Al Kα X-ray source (Surface Sciences, Inc.) was used to make the XPS measurements (analyzing the top ca. 50 Å of the surface). Survey scans (spot 600 μm, resolution 4, window 1000 eV) were used to obtain elemental compositions of the surfaces. High-resolution scans of the carbon 1s photoelectron (spot 600 μm, resolution 2, window 20 eV) were used to obtain the intensity of the ether (C−O) carbon peak (as PEO consists solely of ether carbon). The intensities of the silicon 2p photoelectron were measured (spot 600 μm, resolution 4, window 20 eV) and used in the calculations to obtain the thickness of the protein layer through the attenuation of the silicon signal. In all scans, a flood gun setting of 5 eV was used, as well as a nickel wire mesh held approximately 5 mm over the sample stage, to help prevent charging of the samples. The take-off angles was 35°. All scans of carbon 1s and silicon 2p photoelectrons were peak-fitted using software provided with the instrument. The lowest energy peak in the high-resolution carbon 1s scans was referenced to 285 eV.

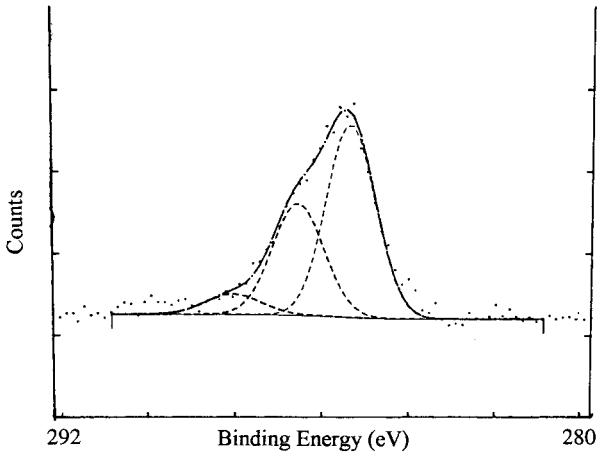

Figure 1. High-resolution carbon scan of an aminosilane-coupled silicon surface.

Results and Discussion

Aminosilane-Coupled Surfaces. Results from ellipsometry show that the aminosilane layer was 7 ± 2 Å. In approximating that the density of the layer is ∼1 g/cm^3, which is the density of the pure silane solution, we can calculate that there are approximately two aminosilane molecules per square nanometer or that the amine concentration is four secondary and two primary amines per square nanometer. An average spacing between amines of 7 Å is entirely sufficient in providing a high grafting density on the surface, since the PEO molecules being grafted are considerably larger than 7 Å in size (the size of a PEO monomer unit is approximately 3 Å). The silane layer was found to be stable for 2 weeks in PBS solution (pH 7.4), as deduced by XPS survey scans, which showed a constant ratio of N/Si intensities.

Thickness of Dried PEO Layer. XPS high-resolution carbon 1s scans were used to quantify the presence of the PEO on the surface when compared to the aminosilane control. Figure 1 shows the high-resolution carbon scan for an aminosilane control surface. The peak shifted 1.1 eV positive of the main C−C peak is indicative of carbon in a single bond with nitrogen (primary, secondary, and tertiary amines all shift the carbon peak equally). The small, highest energy peak is probably due to the presence of carbon dioxide complexed onto the surface. Figures 2 and 3 show the scans for linear PEG 20k and star 3510-coupled surfaces at three different coupling concentrations of tresylated PEO. These scans clearly show the growing intensity of the C−O peak (shifted 1.5 eV from the C−C peak) as the coupling concentration increases, indicating the increasing grafting density of PEO on the surface. In XPS (and ellipsometry) measurements, it is the dried (dehydrated) PEO layer that is being analyzed, where any inhomogeneities on the surface are averaged out as if the surface had a uniform layer. We make the approximation of averaging out over the surface on the basis of several findings. First, the silicon wafers should have no gross anomalies on the surface, as promised by the manufacturer. Second, in coupling the aminosilane to the silicon, it had been found via contact angle analysis, ellipsometry, SEM, and AFM that there are no large distinguishable features on the surface, indicating that the silane covers the surface uniformly.[29,32] Third, AFM has also shown that the PEO-coupled surfaces are uniform with no large anomalies that would

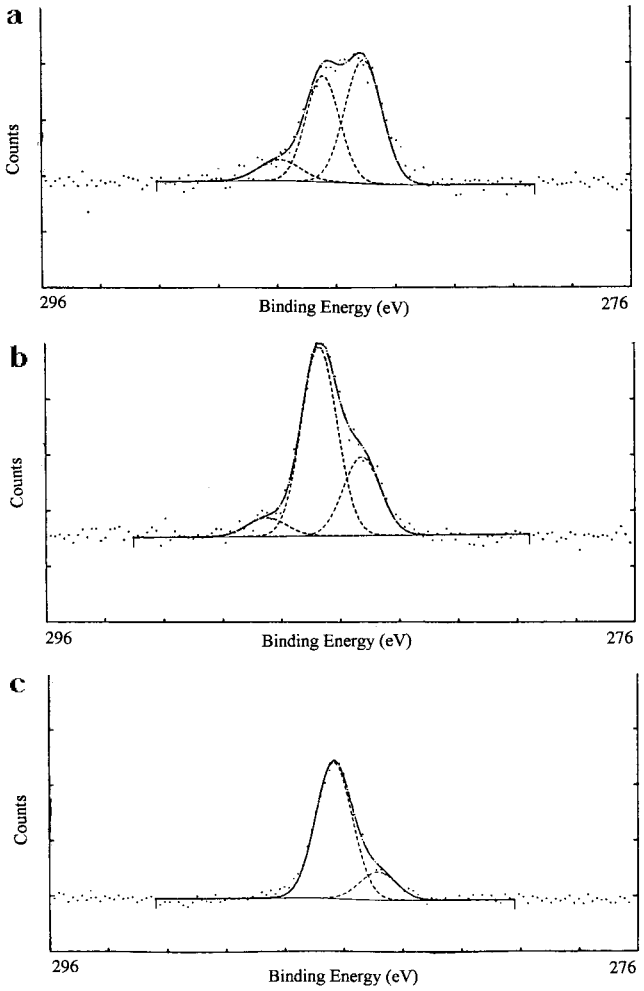

Figure 2. High-resolution carbon scans of PEG 20K-grafted surfaces from three different coupling concentrations: (a) 0.5%; (b) 2%; (c) 15%.

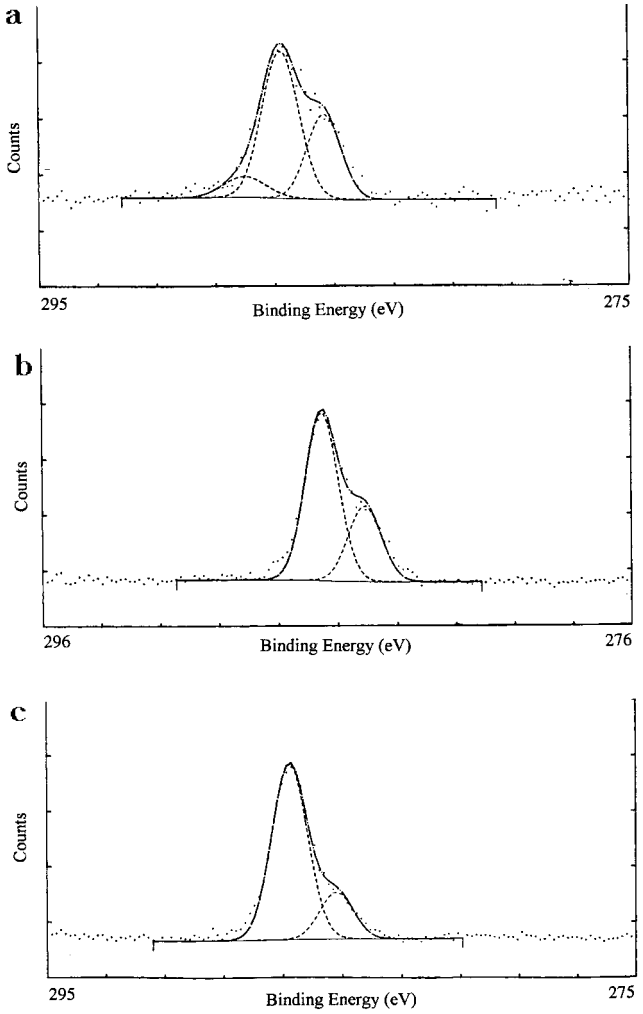

Figure 3. High-resolution carbon scans of star 3510-grafted surfaces from three different coupling concentrations: (a) 0.5%; (b) 7%; (c) 12%.

indicate a clustering or clumping of PEO on the surface.[32] Therefore, we can make approximations regarding the surface characteristics, as in our calculations of grafting density and in our model of the surface.

The intensity of the ether peak can be used to estimate the dried thickness of the PEO layer through the relation

$$\frac{I}{I_0} = 1 - \exp\left(\frac{-d}{\lambda \sin(\theta)}\right) \tag{1}$$

where I is the intensity of the ether peak from a certain PEO layer thickness, I_0 is the intensity from an "infinitely" thick PEO layer, d is the thickness of the PEO layer (Å), λ is the attenuation length of the carbon 1s photoelectron through an organic layer (Å), and θ is the take-off angle used when taking the XPS measurements ($\theta = 35°$). The attenuation length λ was found using the results of Laibinis et al.[33]

$$\lambda\ (\text{Å}) = 9.0 - 0.022(\text{KE})\ (\text{eV}) \tag{2}$$

KE is the kinetic energy of the photoelectron, found by

$$\text{KE (eV)} = 1486.6 - \text{BE} \tag{3}$$

where BE is the binding energy of the photoelectron and 1486.6 eV is the energy of the X-rays. The intensity I_0 was estimated by measuring the intensity I of a well-characterized PEG SAM on gold where the PEG unit consisted of six monomer units. As reported previously,[17] the PEG thickness of such a SAM is 15 Å. Therefore, knowing d, θ, and λ and measuring I, an estimate of I_0 was calculated. This value of I_0 agreed to within 10% of the measured intensity from a pure PEO sample (a PEO thickness greater than 50 Å such that only PEO was detected on the surface). Measurements of I from the PEO samples then yielded the thickness d, using eq 1. On some samples, the nitrogen intensity from the underlying aminosilane layer was greater than 10% of that of the aminosilane surface only, meaning the amine peak was contributing significantly to the C−O peak area. This was generally found for samples treated with tresyl-PEO coupling solutions of concentration less than 1%. For these cases, a fraction of the amine C−N intensity measured on the aminosilane layer (high-resolution scan of C 1s) was subtracted from the C−O intensity measured on the PEO-coupled surface, this fraction equaling the amount of nitrogen measured on the PEO surface (survey scan) relative to that measured on the aminosilane surface. This new value of C−O intensity was then used for the value of I used in eq 1. Overall, the XPS measurements of the PEO layer thickness agreed to within 1−2 Å with the measurements made by ellipsometry. Figure 4 shows the dry PEO thicknesses as a function of tresyl-PEO coupling concentration. For the three linear PEG

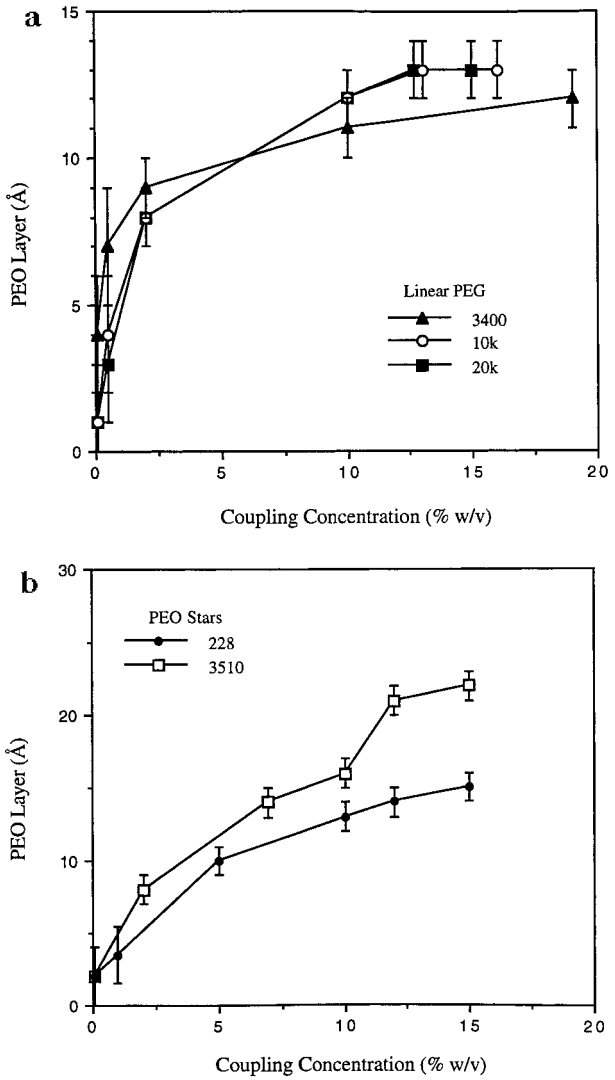

Figure 4. Dry PEO thickness as a function of tresyl-PEO coupling concentration for (a) linear PEG and (b) star PEO.

surfaces, the maximum PEO content grafted to the surface is approximately the same. This has been found to occur for PEG molecular weights greater than 2000 g/mol,[25] when the chain is a full random coil such that excluded volume effects come into play in the grafting of the chains to the surface.

Calculation of Linear PEG Grafting Density. The values of the dry thickness of PEO were used to calculate the grafting density σ of the PEO molecules on the surface. First, the average distance between PEG chains L grafted to the surface was estimated from the dry thickness by

$$L\ (\text{Å}) = \left(\frac{M}{\rho_{\text{dry}}\ h\ N_{\text{A}}}\right)^{1/2} \tag{4}$$

where M is the molecular weight of the PEG chain, ρ_{dry} is the density of the dry PEG layer (assumed constant at 1 g/10^{24} Å^3), h is the thickness of the PEG layer (Å), and N_{A} is Avogadro's number. Therefore, L^2 is the average area occupied by a single PEO molecule on the surface.

The definition of grafting density for linear molecules is defined to be[18]

$$\sigma(\text{linear}) = \left(\frac{a}{L}\right)^2 \tag{5}$$

where a is the size of a monomer unit ($a \approx 3$ Å).[16,21] Therefore, combining eqs 4 and 5, a relationship of σ as a function of M and h is obtained.

$$\sigma(\text{linear}) = \left(\frac{\rho_{\text{dry}} h N_{\text{A}} a^2}{M}\right) \tag{6}$$

The relationship between attained grafting density and tresylated-PEO coupling concentration for the three linear PEG molecules is shown in Figure 5. All three PEG molecules show the same general behavior of a rapid rise in grafting density at low coupling concentrations, with a leveling off such that a maximum grafting density is attained. The dependence of grafting density on PEO coupling concentration can be explained by the strong interactions of the PEO molecules with water molecules in solution. It is believed that there is a specific structure to a hydrated PEO molecular which gives rise to very strong excluded volume effects.[24,34] Isolated, hydrated PEO molecules resist overlapping in aqueous solution, as this would disrupt the water−polymer interactions. However, PEO chains do overlap when forced to at high solution concentrations above c_{crit}, where c_{crit} is the critical concentration marking the onset of chain overlap in solution.

$$c_{\text{crit}} = \left(\frac{M}{N_{\text{A}}\frac{4}{3}\pi R_{\text{G}}{}^3}\right) \tag{7}$$

where R_{G} is the radius of gyration of the linear PEO molecule.[35] Therefore, when grafting linear PEO molecules to a surface at concentrations below c_{crit}, PEO chains do not overlap, and bound PEO chains on a surface exclude other chains from that occupied space. As coupling concentration increases to above c_{crit}, there is significant overlap of PEO chains. There is a higher probability of chains binding to the surface and binding at greater surface densities. At concentrations much above c_{crit} the density of PEO chains bound to the surface becomes high enough such that additional PEO chains can no longer penetrate the bound layer to bind to the surface.[36] This explains the asymptotic behavior seen in Figure 5, as c_{crit} for the PEG molecules, c_{crit}(3400) ≈ 8%, c_{crit}(10K) ≈ 5%, and c_{crit}(20K) ≈ 3 % (w/v), are well below the highest coupling concentrations used. The concentration of PEO at the surface is not necessarily the same as that in the bulk solution, but it is likely that significant chain overlap on the surface was also achieved.[37] It is evident, therefore, that the surface becomes saturated in PEO such that steric hindrance and excluded volume effects result in an increasing resistance for additional PEO chains to penetrate the PEO layer and bind to the surface.[36] It was also believed that the asymptotic behavior shown in Figure 5 may have been a result of hydrolysis of the tresyl groups from the ends of the PEO chains, which is in competition with the binding to surface amines. However, in re-exposing a PEO-coupled surface with fresh tresyl-PEO, there was no measurable difference in the PEO surface content as determined by both XPS and ellipsometry.

The data in Figure 5 also clearly show the dependence of grafting density on PEG molecular weight, with PEG

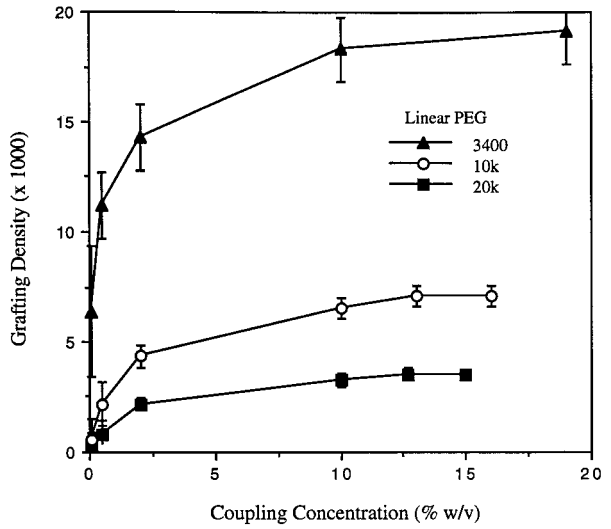

Figure 5. Grafting density as a function of tresylated-PEO coupling concentration for linear PEG 3400, 10K, and 20K.

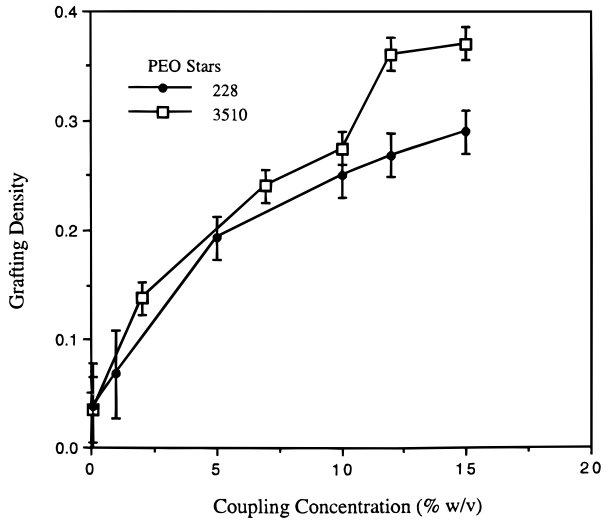

Figure 6. Grafting density as a function of tresylated-PEO coupling concentration for stars 228 and 3510.

3400 attaining the highest densities and PEG 20K attaining the lowest densities. This is again due to excluded volume effects, where a larger PEG molecule has a greater excluded volume and cannot pack as tightly on the surface with equivalent chain spacings (to the same grafting density) as a smaller PEG molecule.

Star PEO Grafting Density. Defining grafting density for the PEO star molecules is not as straightforward as it is for linear PEO molecules. This is because the size of a monomer unit is not feasible to use in the calculation of grafting density for stars, due to the large structural difference between linear and star PEO molecules. Possibly the most appropriate parameter to replace the monomer size a in the grafting density for star PEO surfaces would be the size of the core of the star molecules. However, the core region of a star molecule is very difficult to define, as indicated in much of the literature on star molecules.[27,28,38,39] Therefore, for star molecules, we use the radius of gyration of the star molecules, R_G^{star}, to replace monomer size in the equation for grafting density, since the radius of gyration is a convenient parameter than can be measured or obtained. Therefore, grafting density for a star PEO surface is defined as

$$\sigma(\text{star}) = \left(\frac{R_G^{star}}{L}\right)^2 \tag{8}$$

and the relationship between σ, h, and M for a star is

$$\sigma(\text{star}) = \left(\frac{\rho_{dry} h N_A (R_G^{star})^2}{M}\right) \tag{9}$$

The radius of gyration of a star molecule was estimated using the empirical results set forth by Bauer et al.[26] The relation $\log(R_G^{star}/R_G^{arm})$ versus $\log(f)$ for various star polymers in a good solvent was presented, and from these data we get

$$\log(R_G^{star}/R_G^{arm}) = 0.1312 \log(f) + 0.1910 \tag{10}$$

The value of R_G^{arm} was calculated from eq 8. The average molecular weight of the stars divided by the arm molecular weight yields f. R_G^{star} was then calculated from eq 11 and found to be 80 and 100 Å for stars 228 and 3510, respectively.

Figure 6 shows the attained grafting density as a function of tresyl−star coupling concentration for both star 228 and star 3510. Unlike the behavior of linear PEO, there is no leveling off at a maximum grafting density at large concentrations. Instead, σ continues to increase even at the highest coupling concentrations. One hypothesis to account for these results again has to do with the critical concentration of the molecules in solution: $c_{crit}(228) \approx 15\%$ and $c_{crit}(3510) \approx 13.5\%$. At the highest coupling concentration of 15%, both stars have just reached the point of overlap. Therefore, from this point onward is where we would expect grafting density to reach a maximum due to steric repulsion and excluded volume effects on the surface. The extremely large values of c_{crit} for the stars are testimony to how dense the stars are, where such high concentrations are needed before the stars are forced to interpenetrate one another.

Protein Adsorption on PEO Surfaces. The thickness of the layer of adsorbed protein was determined by analyzing the attenuation of the silicon 2p photoelectron signal in an XPS scan, as referenced to the equivalent PEO surface not contacted with protein. The attenuation of a photoelectron signal due to an overlayer is described by the equation

$$\frac{I}{I_0} = \exp\left(\frac{-d}{\lambda \sin\theta}\right) \tag{11}$$

where I is the intensity of Si 2p with a protein overlayer, I_0 is the intensity of Si 2p with no protein overlayer, d is the thickness of the protein overlayer (Å), λ is the attenuation length of Si 2p through an organic overlayer (estimated to be 38.5 Å from eqs 2 and 3), and θ is the take-off-angle used in taking the measurements ($\theta = 35°$). Therefore, by measuring I and I_0 in an XPS scan, the protein thickness d was calculated. As the thickness of the silicon oxide layer on the wafers was measured to be greater than 200 Å, any changes in the Si 2p intensity would be due to changes in overlayer thickness only, making possible the use of eq 12. Measurements of protein adsorption by XPS in this way agreed very well with ellipsometry measurements.

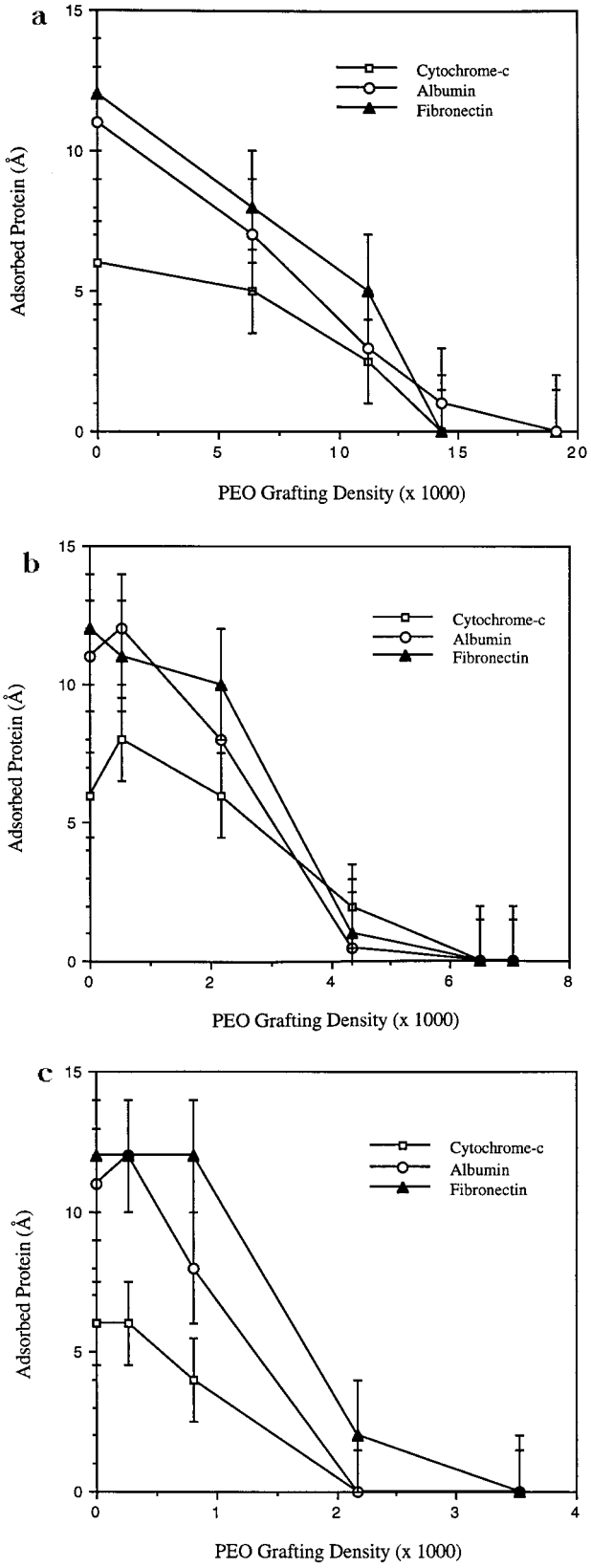

Figure 7. Protein adsorption as a function of grafting density on (a) PEG 3400, (b) PEG 10K, and (c) 20K surfaces.

Protein Adsorption on Linear PEG Surfaces. Figure 7 shows adsorption as a function of PEG grafting density for cytochrome-*c*, albumin, and fibronectin on surfaces grafted with linear PEG 3400, 10K, and 20K. Again, these three proteins were chosen because they span a wide range of protein size, such that adsorption as a function of protein size could also be investigated. (Zero protein adsorption corresponds to less than 1 ng/cm^2 of protein.) There are several common features in the adsorption on all three PEG surfaces. There is a small region of high adsorption at low PEO coverage, followed by a rapid decline in adsorption with PEO coverage until it reaches zero measurable adsorption at the highest grafting densities. What is interesting to note is that the three proteins change from maximum to minimum adsorption in roughly the same range of grafting densities on each PEG surface, despite the large difference in protein size. In fact, albumin and fibronectin show very similar adsorption, despite the large difference in their molecular weights. This is probably due to the small 25 Å width characteristic of fibronectin, causing it to behave as a protein whose effective size is similar to that of albumin. In addition, on all three PEG surfaces, the amount of protein adsorbed at a given grafting density generally correlates with the size of the protein, with fibronectin showing the greatest adsorption, followed by albumin and then cytochrome-*c*. For an equal area, a large protein adsorbed to the surface in a single layer is more total adsorbed protein (mass/area) than a layer of a small protein due to the layer of the larger protein being of greater thickness. The fact that fibronectin does not exhibit much larger thicknesses when compared to albumin and cytochrome-*c*, despite its much larger mass, suggests that fibronectin, having a rodlike shape where the other two are spherical, lies down on the surface with its long axis parallel to the surface.

An important conclusion to draw from the results in Figure 7 is that there appears to be no specific PEO molecular weight, or universal range of PEO grafting densities, that is necessary for the prevention of protein adsorption, at least in the ranges of protein sizes and PEG molecular weights studied. Instead, for a given PEO molecular weight there is a specific grafting density above which protein adsorption is prevented. In an extensive study conducted by Abbott et al.[40−43] where PEO−protein interactions in two-phase dextran systems were studied, it was found that, for protein sizes on the order of or greater than the size of the PEO coil, the PEO chain will effectively exclude the protein from its volume. For protein sizes considerably smaller than the size of the PEO coil, however, the protein can penetrate the PEO volume without much disruption of the PEO configuration. These results agree with the findings of Antonsen and Hoffman.[34] Through an extensive DSC analysis, they uncovered an association of water molecules with a PEO chain and its dependence on PEO molecular weight. Disruption of this association by a protein leads to a steric repulsion, causing a rejection of the protein and a returning of the PEO coil to its original configuration. In the data we present in this paper, the sizes of all three proteins are roughly equal to or greater than the size of the PEO molecules. Therefore the proteins interact with the PEO chains in a similar manner and thus exhibit similar adsorption behavior. We discuss these issues in more detail in the next section where a model of protein adsorption on the PEO-grafted surfaces is presented.

Protein Adsorption on Star PEO Surfaces. Figure 8 shows protein adsorption as a function of grafting density for cytochrome-*c*, albumin, and fibronectin on the two star PEO surfaces. Similar features to those outlined on linear PEG surfaces can be seen in the

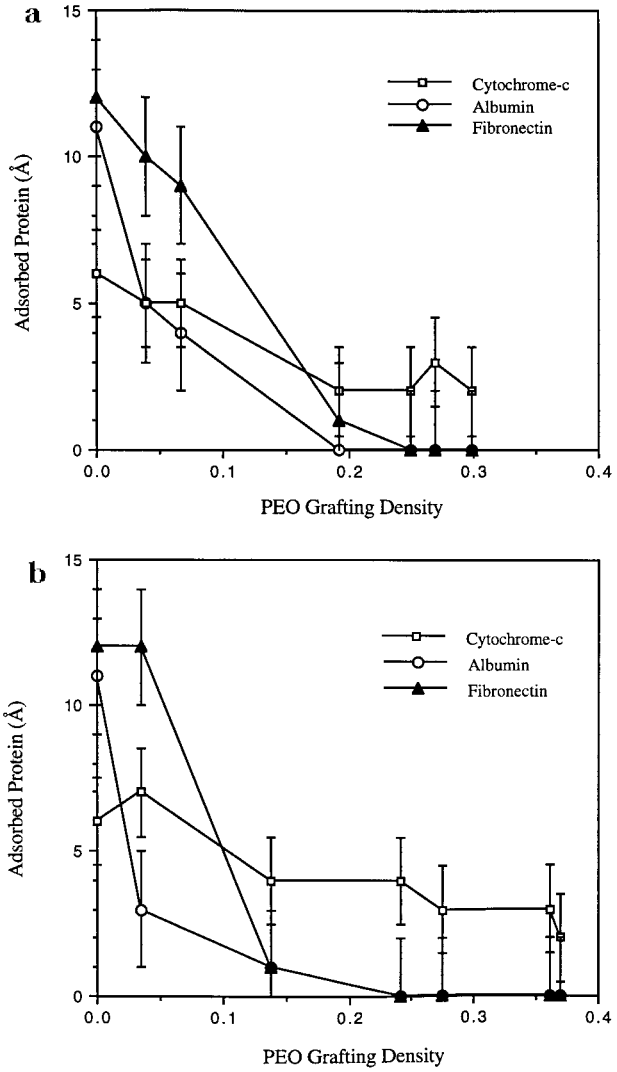

Figure 8. Protein adsorption as a function of grafting density on (a) star 228 and (b) star 3510 surfaces.

adsorption of albumin and fibronectin. They show similar values in adsorption and exhibit a rapid decline in adsorption in the same range of star grafting density for each of the star surfaces. The most glaring feature of the protein adsorption on both star surfaces is the continued adsorption of cytochrome-*c* at all grafting densities. This can most likely be attributed to the hard-sphere character of the star molecules. On average, the star molecules are over two to three times more dense in PEO than a linear molecule of equivalent hydrodynamic size. Therefore, the site of a grafted star molecule presents a more effective barrier by itself in preventing proteins from adsorbing at that site than a linear, randomly coiling molecule. For a star surface, the sites available for protein adsorption are therefore only located between the grafted molecules. When these open spaces between star molecules become smaller than the effective size of the protein, then proteins can no longer adsorb. This topic is further discussed in the next section.

Simple Model of the Surface. We present the following physical model to explain, qualitatively, the dependence of protein adsorption on PEO grafting density. It is based mainly on the spatial arrangement of PEO molecules relative to one another on the surface. Energies of interaction between protein and PEO do not enter into it, although certain qualitative arguments can

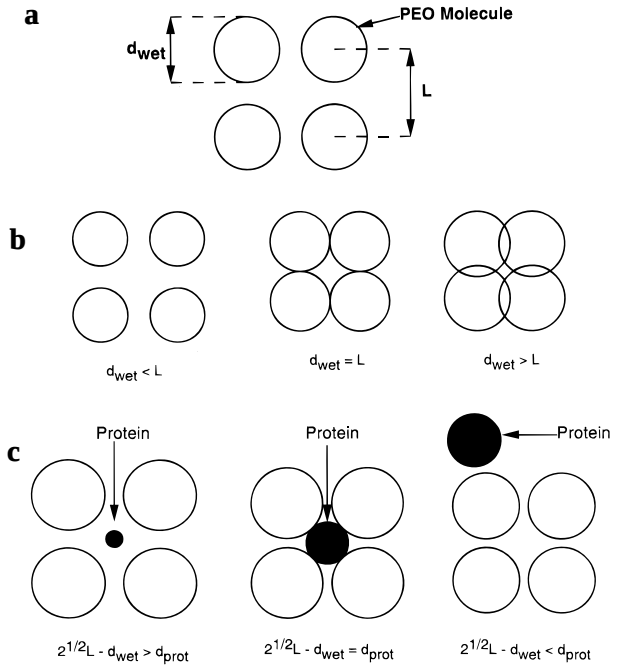

Figure 9. 2-D model (a) of PEO chains grafted on a surface and (b) depicting the degree of chain overlap and (c) correlating chain spacing with protein size.

be made. When applying this model to the experimental findings presented, we find that it explains extremely well the observed trends seen in the adsorption of the three proteins on both the linear and star PEO-grafted surfaces.

(a) Defining the Parameters. We describe a surface where PEO molecules are bound in a 2-D lattice structure where a unit cell is defined to have length L (see Figure 9a). Therefore, L^2 is the area occupied by one hydrated molecule, including half the open space around it if it does not overlap with any other molecules. The diameter of the hydrated molecule is d_{wet}, defined to be twice the radius of gyration R_G of the PEO molecule: $d_{wet}(\text{linear}) = 2R_G^{linear}$, $d_{wet}(\text{star}) = 2R_G^{star}$. The characteristic sizes of the proteins d_{prot} are well-known, and all values of d_{wet} and d_{prot} are given in Table 1. Note that due to the nonglobular, rodlike shape of fibronectin, a characteristic size of the protein was chosen to be its radius of gyration as calculated by

$$R_G^2(\text{rod}) = \frac{l_r^2}{12} \tag{12}$$

where l_r is the length of the rod.

(b) PEO Chain Overlap and Protein Adsorption on Linear PEG Surfaces. To characterize PEO chain spacing, we focus on the degree of chain overlap on the surface, and thus the degree of surface coverage provided by the PEO layer. As depicted in Figure 9b, when $d_{wet} < L$, the PEO molecules do not overlap and there is significant open space on the surface available for protein adsorption. When $d_{wet} = L$, the PEO chains are just starting to overlap with the closing off of open space. When $d_{wet} = 2^{1/2}L$, the surface is fully covered by a layer of PEO with no open space available for direct protein adsorption. Concerning these conditions, we would possibly expect transitions in protein adsorption in going from the first to the third condition of PEO grafting density.

Table 1. Values of Molecular Weight, d_{wet}, and d_{prot}, for the Proteins and Linear and Star PEO Molecules

PEO	M (g/mol)	d_{wet} (Å)	protein	M (kD)	d_{prot} (Å)
3400	3 400	48	cyt-*c*	12	34, globular
10K	10 000	88	alb	68	72, globular
20K	20 000	128	fib	500	600 long, 25 wide, rodlike, $R_G = 165$
star 3510	350 000 ($M_{arm} = 5200$)	200			
star 228	200 000 ($M_{arm} = 10\,000$)	160			

Table 2. Values of Grafting Density for When $d_{wet} = L$ and $d_{wet} = 2^{1/2}L$ for Linear PEG Surfaces

PEG	$\sigma(d_{wet}=L)$	$\sigma(d_{wet}=2^{1/2}L)$
3400	0.003 19	0.006 38
10K	0.001 18	0.002 36
20K	0.000 56	0.001 12

When describing the protein adsorption on the linear PEG surfaces, we can correlate adsorption with grafting density by noting the values of grafting density σ for which $d_{wet} = L$ and $d_{wet} = 2^{1/2}L$. As stated above, we would expect transitions in the adsorption behavior to occur somewhere in the vicinity of these points. From eqs 5 and 6, the values of $\sigma(d_{wet}=L)$ and $\sigma(d_{wet}=2^{1/2}L)$ were calculated and are given in Table 2. The values are small, at the low end of the grafting densities achieved on the PEG surfaces. The surface easily becomes covered by a nonoverlapping monolayer of PEO molecules. When we correlate these values of σ to the adsorption data shown in Figure 7, the protein adsorption is indeed starting to fall off at these low values of σ. However, just covering the surface with linear PEO molecules is not sufficient to prevent proteins from reaching the surface, as seen by the significant adsorption at these values of grafting density as well as the continued, although lower, adsorption at more intermediate grafting densities. Szleifer[21] saw similar results in a theoretical analysis of protein adsorption to PEO-layered surfaces. It was found that proteins are able to work their way through the PEO layer to sit on the underlying surface in between grafted chains, reaching a compromise between conformational entropy of the grafted polymers, polymer−protein repulsions, and attraction of the protein for the surface. Depending on the grafting density of the PEO chains, the adsorbed protein will deform the surrounding grafted chains to some degree. As such, the greater the grafting density, the greater the deformation and the less favorable the overall interaction, which results in lower protein adsorption. The results of Jeon et al.[22,23] are also in agreement, where they concluded from their theoretical study that grafting density is more important than PEO molecular weight in preventing protein adsorption.

One can note from correlating Table 2 with Figure 7 that the adsorption begins to decline only when the PEO chains start to fully overlap, at grafting densities greater than $\sigma(d_{wet}=2^{1/2}L)$. An important feature in the adsorption is the point at which the onset of minimum adsorption occurs. On each of the PEG surfaces, the adsorption of the three proteins becomes negligible at about the same value of σ, which is near the highest grafting density achieved on the surface. An estimate of the grafting density at these minimum adsorption points is $\sigma^*(3400) \approx 0.014$, $\sigma^*(10K) \approx 0.0043$, and $\sigma^*(20K) \approx 0.0022$ for each of the three linear PEG surfaces, respectively. In calculating the corresponding overlap, we find it is approximately the same on all three PEG surfaces, $d_{wet} \approx 2L$. Therefore, extensive chain overlap to the point where PEO chains are roughly doubled up on the surface is significant in preventing protein adsorption. Furthermore, at this overlap, the chain spacing is approximately equal to the radius of gyration of the PEG molecule, $L \approx R_G$ linear. This exact spacing is known for polymer brushes as marking the point on the surface where the excluded volume of the grafted chains would cause them to extend away from the substrate surface, resulting in chain stretching.[18,44,45] It is therefore not surprising that, under these conditions, proteins will not be able to sit on the surface. If the chains are stretching in order to avoid themselves and surrounding chains, then it follows that they would rebel against being further deformed by an adsorbed protein, agreeing again with the findings of Szeifler.[21] In fact, the values of σ^* lie in the "knee" of the curve of grafting density versus tresyl-PEG coupling concentration (see Figure 5), marking the point where the maximum PEG grafting density is almost reached. This indicates that additional PEG chains themselves are beginning to have difficulty adding to the already dense PEO layer.

The above conclusion that extensive chain overlap is needed on linear PEO surfaces for preventing protein adsorption also explains, in part, the lack of dependence of protein adsorption on protein size. For example, given the large size of fibronectin, we would maybe expect to see a rapid, early decrease in adsorption (i.e., at low grafting densities) compared to those for the other two smaller proteins, with fibronectin ultimately being the first to be excluded from the surface. We do not observe this behavior, but rather we see the decline in adsorption for all three proteins occurring over the same range of grafting densities. This is possibly due to a relatively equal trade-off between the energy cost required for a protein to "fit in" on the surface and the energy gain through the attractive interaction between the protein and the surface. The larger the protein, the greater the total surface attraction, but also the greater the extent that PEO chains are compressed, and thus the greater the repulsion.[22,23] These conclusions agree with those of Abbott et al.[40,41] for $d_{prot} \geq d_{PEO}$, except now there is the added interaction of the protein with the underlying surface. As stated by Szeifler[21] and others,[22,24,25,40] there are many factors that can influence the adsorption of a specific protein to a surface, such as charged groups and hydrophobic patches on the protein, the shape of the native protein conformation, as well as the nature of the adsorbing surface. Thus, it is a complex issue such that subtle differences may be observed for different proteins. Our results show only an example of these PEO/protein interactions.

(c) Protein Adsorption on PEO Star Surfaces. The same analysis that was used for protein adsorption on linear PEG surfaces was applied to the PEO star surfaces. Values of σ when $d_{wet} = L$ (start of the PEO star overlap) and $d_{wet} = 2^{1/2}L$ (overlap of stars such that all open space is covered with PEO) are given in Table 3. In correlating the values of $\sigma(d_{wet} = L)$ to the protein adsorption data shown in Figure 8, it is clear that the initial point of star overlap was reached for both star surfaces, since the grafting densities of stars 228 and

Table 3. Values of Grafting Density When $d_{wet} = L$ and $d_{wet} = 2^{1/2}L$ for PEO Star Surfaces

	$\sigma(d_{wet}=L)$	$\sigma(d_{wet}=2^{1/2}L)$
star 228	0.250	0.500
star 3510	0.250	0.500

Table 4. Values of Grafting Density when $2^{1/2}L - d_{wet} = d_{prot}$ for PEO Star Surfaces

	cyt-*c*	alb	fib
star 228	0.347	0.237	0.121
star 3510	0.378	0.265	0.138

3510 reached and exceeded 0.250. At this value of σ, both fibronectin and albumin have nearly reached zero adsorption, whereas cytochrome-c still shows significant adsorption. The value of $\sigma(d_{wet}=2^{1/2}L) = 0.500$ for both star 228 and star 3510 indicates that neither star surface has reached full coverage of PEO, since the highest grafting densities achieved were only 0.289 for star 228 and 0.370 for star 3510. Therefore, there are open spaces still existing on the surface, unlike the linear PEG surfaces.

At this point we introduce a third PEO surface condition in our model of the PEO surfaces, which we describe as

$$\frac{d_{prot}}{2^{1/2}L - d_{wet}} \tag{13}$$

This condition takes into account the size of the adsorbing protein and how it relates to the open space on the surface in the center of the unit cell, approximated as $2^{1/2}L - d_{wet}$ (see Figure 9c). When this open space is greater than the size of the protein, then we expect protein adsorption to occur. When the two are equal, we may expect to see the start of decreased protein adsorption. When the protein size is greater than the open space at $2^{1/2}L - d_{wet} < d_{prot}$, then we expect to see reduced protein adsorption. The condition $2^{1/2}L - d_{wet} = d_{prot}$, where we may expect to see a transition in protein adsorption behavior, can occur at any degree of PEO chain overlap depending on the size of the PEO and the size of the protein. We can therefore calculate values of $\sigma(2^{1/2}L - d_{wet} = d_{prot})$ where we would expect to see a change in the adsorption of a particular protein. These values of grafting density for the three adsorbing proteins are given in Table 4.

In correlating these values of σ in Table 4 to the data in Figure 8, several observations can be made. First, the open spaces on the surface become smaller than the size of albumin at $\sigma \approx 0.237$ on star 228 and $\sigma \approx 0.265$ on star 3510, which correlates with the drop to zero adsorption at these grafting densities in Figure 8. The drop to zero at this point and not at a higher value of σ indicates that the protein cannot easily move or compress the star PEO chains out of the way so as to diffuse and adsorb into a space smaller than its size, whereas it can do this with linear PEG prior to the point σ^*. This supports the notion of star molecules behaving as hard spheres, being severalfold more dense in polymer than linear molecules of the same effective diameter. Therefore the entropic cost in compressing the star chains is much greater than that for a linear molecule. The PEO star molecules thus define a rigid-wall pore such that when the diameter of this pore becomes smaller than the protein diameter, the protein is excluded.

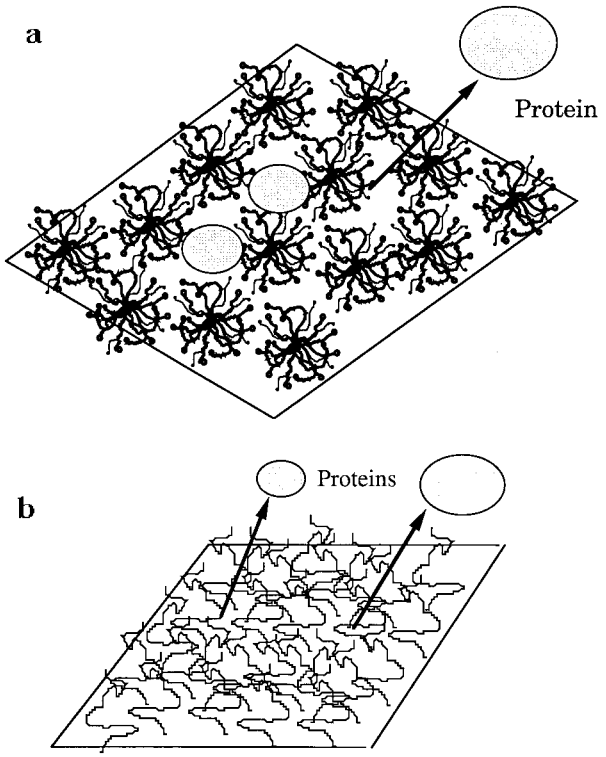

Figure 10. Depiction of protein adsorption on (a) PEO star and (b) linear PEG surfaces.

Fibronectin does not reach zero adsorption at $\sigma \approx 0.121$ (star 228) or 0.138 (star 3510), as the values in Table 4 indicate. One possibility for this is that the choice of the radius of gyration of fibronectin as an estimate of d_{prot} may not have been the most appropriate parameter to use in the model. As seen in the adsorption on linear PEG surfaces, fibronectin seems to behave like a protein with an effective size similar to that of albumin, which is in agreement with the adsorption behavior of fibronectin on star surfaces shown in Figure 8.

The values of grafting density where $2^{1/2}L - d_{wet} = d_{prot}$ for cytochrome-*c* on the star 228 and star 3510 surfaces are greater than the maximum grafting densities achieved on both star surfaces. Therefore, the condition where the open spaces between star molecules are smaller than the size of cytochrome-*c* has *not* yet been reached. This explains the continued, although decreased, adsorption of cytochrome-*c* where albumin and fibronectin no longer adsorb. If a value of σ greater than 0.289 or 0.370 was obtained on the star 228 or 3510 surfaces, respectively, then a drop to zero in the cytochrome-*c* adsorption would probably be observed. Figure 10a is a possible picture of the star surface that depicts the continued adsorption of cytochrome-*c*. Here, the entire space occupied by the star molecule is excluded to the protein. This is in contrast to that of a linear PEG surface, which is pictured in Figure 10b, where the space occupied by the PEG molecule is not impenetrable to proteins until significant chain overlap is achieved.

Overall, the protein adsorption of the three proteins were similar on both star 228 and star 3510 surfaces, despite the differences in functionality and arm molecular weight of the two star species. This is probably because both stars are in the limit of behaving like hard spheres. Therefore, a protein perceives both surfaces

similarly, where it can only adsorb in the open spaces between star molecules.

Complete coverage of the surface with star PEO of either kind was not achieved in the experiments presented here, but this is not to say that it cannot be achieved. As stated earlier, the highest coupling concentration used for the binding of star molecules was just at the point of chain overlap, which correlates well with the small chain overlap observed on the star-grafted surfaces as shown by the model. Higher concentrations would force the molecules to interpenetrate. This would increase the molecular overlap on the surface and decrease the available open space between molecules. Therefore, the potential exists for increased star coverage on the surface and the subsequent prevention of adsorption of even very small proteins like cytochrome-*c*.

Summary

In this paper, we presented a method for creating PEO-grafted surfaces that were used for analyzing the dependence of protein adsorption on PEO grafting density, molecular weight, PEO molecular type, and protein size. The grafting density of PEO on the surface was determined through a measurement of the dry thickness of the grafted PEO layer. The adsorption of three proteins of varying sizes was then measured on these PEO surfaces. Analysis of the surfaces was performed by XPS and ellipsometry, which in general showed good agreement between measurements. A model of the surface based on the spatial arrangement of the PEO chains helped explain the protein adsorption behavior that was observed.

On linear PEG surfaces, it was found that simply covering the surface with a nonoverlapping monolayer of PEO was not sufficient to significantly prevent protein adsorption. Instead, complete coverage of the surface with grafted polymer to the point where the chains are roughly half-overlapping (i.e., $L \approx R_G^{linear}$) is important for the nonadsorption of proteins. This needed degree of overlap appeared to be independent of PEO molecular weight and protein size, at least in the range of PEO molecular weights and protein sizes studied (i.e., $d_{prot} \geq d_{PEO}$). However, to achieve this chain overlap, higher grafting densities are needed for smaller PEG molecular weights, indicating that there is a specific dependence of protein adsorption on grafted PEO molecular weight. Protein adsorption is thus not solely dependent on values of grafting density but on values of grafting density for a specific molecular weight of grafted PEO. As explained by Szleifer,[21] this phenomenon is caused when there is an attractive interaction between PEO and the substrate surface. That is, if there were not this attractive interaction, then the protein adsorption behavior would have been the same in the *same* range of grafting density despite the differences in linear PEO molecular weight.

In contrast to surfaces grafted with linear PEO, star PEO-grafted surfaces can prevent adsorption of larger proteins even though open spaces exist between bound molecules. Adsorption is prevented as long as these spaces are smaller than the effective size of the protein. The latter behavior is a consequence of the hard-sphere character of the PEO stars. They are much more concentrated in polymer segments than linear chains of equivalent molecular weight or equivalent size, which leads to markedly higher steric repulsion forces if they are compressed by a protein. Therefore, the star molecules themselves are sufficient on their own, without the need for overlap, in preventing proteins from adsorbing to the space they occupy on a surface. In order to eliminate the open spaces to prevent adsorption of even small proteins, it would be necessary to utilize high concentrations of PEO star molecules, above c_{crit}, during the surface grafting process. This would force interpenetration of the arms on contiguous stars and thus reduce the open space on the surface. As stated earlier in the paper, these results are only one example of the possible adsorption behavior of proteins on PEO surfaces. As many factors such as the specific protein or adsorbing surface can come into play, then some differences in adsorption behavior may be found when different systems are studied.

Acknowledgment. We would like to thank Professors Paul E. Laibinis and Linda G. Griffith of the Department of Chemical Engineering at MIT for their helpful input in doing this study.

References and Notes

(1) Merrill, E. W.; Salzman, E. W. *ASAIO J.* **1983**, *6*, 60−66.
(2) *Poly(Ethylene Glycol) Chemistry: Biotechnical and Biomedical Applications*, Harris, J. M., Ed.; Plenum Press: New York, 1992.
(3) Bergstrom, K.; Holmberg, K.; Safrani, A.; Hoffman, A. S.; Edgell, M. J.; Kozlowski, A.; Hovanes, B.A.; Harris, J. M. *J. Biomed. Mater. Res.* **1992**, *26*, 779−786.
(4) Gombotz, W. R.; Guanghui, W.; Horbett, T. A.; Hoffman, A. S. *J. Biomed. Mater. Res.* **1991**, *25*, 1547−1562.
(5) Han, D. K.; Park, K. D.; Ryu, G. H.; Kim, U. Y.; Min, B. G.; Kim, Y. H. *J. Biomed. Mater. Res.* **1996**, *30*, 23−30.
(6) Huang, S.-C.; Caldwell, K. D.; Lin, J.-N.; Wang, J.-K.; Herron, J. N. *Langmuir* **1996**, *12*, 4292−4298.
(7) Lee, J. H.; Kopecek, J.; Andrade, J. D. *J. Biomed. Mater. Res.* **1989**, *23*, 351−368.
(8) Malmsten, M.; Van Alstine, J. M. *J. Colloid Interface Sci.* **1996**, *177*, 502−512.
(9) Österberg, E.; Bergström, K.; Holmberg, K.; Riggs, J. A.; Van Alstine, J. M.; Schuman, T. P.; Burns, N. L.; Harris, J. M. *Colloids Surf., A* **1993**, *77*, 159−169.
(10) Desai, N. P.; Hubbell, J. A. *Biomaterials* **1991**, *12*, 144−152.
(11) Drumheller, P. D.; Hubbell, J. A. *J. Biomed. Mater. Res.* **1995**, *29*, 207−216.
(12) Ferruti, P.; Penco, M.; D'Addato, P.; Ranucci, E.; Deghenghi, R. *Biomaterials* **1995**, *16*, 1423−1431.
(13) Morra, M.; Occhiello, E.; Garbassi, F. *Clin. Mater.* **1993**, *14*, 255−265.
(14) Shard, A. G.; Davies, M. C.; Tendler, S. J. B.; Nicholas, C. V.; Purbrick, M. D.; Watts, J. F. *Macromolecules* **1995**, *28*, 7855−7862.
(15) Silver, J. H.; Myers, C. W.; Lim, F.; Cooper, S. L. *Biomaterials* **1994**, *15*, 695−704.
(16) Prime, K. L.; Whitesides, G. M. *J. Am. Chem. Soc.* **1993**, *115*, 10714−10721.
(17) Pale-Grosdemange, C.; Simon, E. S.; Prime, K. L.; Whitesides, G. M. *J. Am. Chem. Soc.* **1991**, *113*, 12−20.
(18) De Gennes, P. G. *Macromolecules* **1980**, *13*, 1069−1075.
(19) Hommel, H.; Halli, A.; Touhami, A.; Legrand, A. P. *Colloids Surf., A* **1996**, *111*, 67−74.
(20) Milner, S. T. *Science* **1991**, *251*, 905−914.
(21) Szleifer, I. *Biophys. J.* **1997**, *72*, 595−612.
(22) Jeon, S. I.; Lee, J. H.; Andrade, J. D.; de Gennes, P. G. *J. Colloid Interface Sci.* **1991**, *142*, 149−158.
(23) Jeon, S. I.; Andrade, J. D. *J. Colloid Interface Sci.* **1991**, *142*, 159−166.
(24) Lim, K.; Herron, J. N. In *Poly(Ethylene Glycol) Chemistry: Biotechnical and Biomedical Applications*; Harris, J. M., Ed.; Plenum Press: New York, 1992; p 29.
(25) Gölander, C.-G.; Herron, J. N.; Lim, K.; Claesson, P.; Stenius, P.; Andrade, J. D. In *Poly(Ethylene Glycol) Chemistry: Biotechnical and Biomedical Applications*; Harris, J. M., Ed.; Plenum Press: New York, 1992; p 221.
(26) Bauer, B. J.; Fetters, L. J.; Graessley, W. W.; Hadjichristidis, N.; Quack, G. F. *Macromolecules* **1989**, *22*, 2337−2345.

(27) Daoud, M.; Cotton, J. P. *J. Phys. (Paris)* **1982**, *43*, 531−538.
(28) Douglas, J. F.; Roovers, R.; Freed, K. F. *Macromolecules* **1990**, *23*, 4168−4180.
(29) Stenger, D. A.; Georger, J. H.; Dulcey, C. S.; Hickman, J. J.; Rudolph, A. S.; Nielsen, T. B.; McCort, S. M.; Calvert, J. M. *J. Am. Chem. Soc.* **1992**, *114*, 8435−8442.
(30) Nilsson, K.; Mosbach, K. *Biochem. Biophys. Res. Commun.* **1981**, *102*, 449−457.
(31) Nilsson, K.; Mosbach, K. *Methods Enzymol.* **1984**, *104*, 56−69.
(32) Irvine, D. J.; Mayes, A. M.; Satija, S. K.; Barker, J. G.; Sofia-Allgor, S. J.; Griffith, L. G. *J. Biomed. Mater. Res.*, in print.
(33) Laibinis, P. E.; Bain, C. D.; Whitesides, G. M. *J. Phys. Chem.* **1991**, *95*, 7017−7021.
(34) Antonsen, K. P.; Hoffman, A. S. In *Poly(Ethylene Glycol) Chemistry: Biotechnical and Biomedical Applications*; Harris, J. M., Ed.; Plenum Press: New York, 1992; p 15.
(35) *Principles of Polymer Chemistry*; Flory, P. J., Ed.; Cornell University Press: Ithaca, NY, 1953.
(36) Kopf, A.; Baschnagel, J.; Wittmer, J.; Binder, K. *Macromolecules* **1996**, *29*, 1433−1441.
(37) Auroy, P.; Auvray, L.; Leger, L. *Macromolecules* **1991**, *24*, 2523−2528.
(38) Boothroyd, A. T.; Squires, G. L.; Fetters, L. J.; Rennie, A. R.; Horton, J. C.; de Vallera, A. M. B. G. *Macromolecules* **1989**, *22*, 3130−3137.
(39) Grest, G. S.; Kremer, K.; Witten, T. A. *Macromolecules* **1987**, *20*, 1376−1383.
(40) Abbott, N. L.; Blankschtein, D.; Hatton, T. A. *Macromolecules* **1991**, *24*, 4334−4348.
(41) Abbott, N. L.; Blankschtein, D.; Hatton, T. A. *Macromolecules* **1992**, *25*, 3917−3931.
(42) Abbott, N. L.; Blankschtein, D.; Hatton, T. A. *Macromolecules* **1992**, *25*, 3932−3941.
(43) Abbott, N. L.; Blankschtein, D.; Hatton, T. A. *Macromolecules* **1992**, *25*, 5192−5200.
(44) Alexander, S. *J. Phys. (Paris)* **1977**, *38*, 983−987.
(45) Carignano, M. A.; Szleifer, I. *Macromolecules* **1995**, *28*, 3197−3204.

MA971016L